Available online at www.sciencedirect.com
SCIENCE DIRECT®
Journal of Sound and Vibration 270 (2004) 587–610
JOURNAL OF SOUND AND VIBRATION
www.elsevier.com/locate/jsvi

Propagation of Lamb waves in a transversely isotropic piezothermoelastic plate

J.N. Sharma*, Mohinder Pal

Department of Applied Sciences, National Institute of Technology, Deemed University, Hamirpur 177005, India

Received 13 August 2002; accepted 29 January 2003

Abstract

The propagation of Lamb waves in a homogeneous, transversely isotropic, piezothermoelastic plate subjected to charge- and stress-free, thermally insulated or isothermal boundary conditions, is investigated. Secular equations for the plate in closed form and isolated mathematical conditions for symmetric and antisymmetric wave mode propagation in completely separate terms are derived. It is shown that motion of purely transverse (SH) mode gets decoupled from rest of the motion and remains unaffected due to piezoelectric, pyroelectric and thermal effects. At short wavelength limits, the secular equations for symmetric and skew symmetric waves reduce to Rayleigh surface wave frequency equation, because a finite plate in such situation behaves like a semi-infinite medium. The amplitudes of dilatation, temperature change and electrical potential have also been computed during the symmetric and skew symmetric mode of vibrations of the plate. Finally, numerical solution of various secular equations and other relevant relations is carried out for cadmium-selenide (6 mm class) material. The dispersion curves, attenuation coefficients and amplitudes of dilatation, temperature change and electrical potential for symmetric and antisymmetric wave modes are presented graphically in order to illustrate and compare the analytical results. The theory and numerical computations are found to be in close agreement. The various wave characteristics are found to be more stable and realistic in the presence of piezoelectric and pyroelectric effects than in the absence of such effects, thereby making such materials more viable for practical applications and use.
© 2003 Elsevier Ltd. All rights reserved.

1. Introduction

Mindlin [1] first proposed a thermo-piezoelectricity theory. He also derived the governing equations of a thermo-piezoelectric plate [2]. Nowacki [3–5] has explored the physical laws for the thermo-piezoelectric materials. Chandrasekharaiah [6,7] has generalized Mindlin's theory of

*Corresponding author. Tel.: +91-1972-23296; fax: +91-1972-23834.
E-mail address: jns@recham.ernet.in (J.N. Sharma).

0022-460X/03/$ - see front matter © 2003 Elsevier Ltd. All rights reserved.
doi:10.1016/S0022-460X(03)00093-2

thermo-piezoelectricity to account for the finite speed of propagation of thermal disturbances. Several investigators [8–14] have studied the propagation of waves in plates, cylinders and general three-dimensional bodies that are made of thermo-piezoelectric materials. Tauchert [15] has recently applied thermo-piezoelectricity theory to composite plate. Tang and Xu [16] derived the general dynamic equations, which include mechanical, thermal and electric effects, based on the anisotropic composite laminated plate theory. They also obtained analytical dynamical solutions for the case of general forces acting on a simply supported piezothermoelastic laminated plate and harmonic responses to temperature variation and electric field have been examined as a special case.

Recently, resurgent interest in Lamb waves was partially initiated by its application of multisensors [17–19]. Schoch [20] derived the dispersion relation for leaky Lamb waves for an isotropic plate immersed in an inviscid liquid. Incidentally, the dispersion equations also have an interface wave solution whose velocity is slightly less than the bulk sound velocity in the liquid and most of the energy is in the liquid. It is often called the Scholte wave after Scholte [21]. Watkins et al. [22] calculated the attenuation of Lamb waves in the presence of an inviscid liquid using an acoustic impedance method. Wu and Zhu [23] studied the propagation of Lamb waves in a plate bordered with inviscid liquid layers on both sides. The dispersion equations of this case were derived and solved numerically. Zhu and Wu [24] derived the dispersion equations of Lamb waves of a plate bordered with viscous liquid layer or half-space viscous liquid on both sides. Numerical solutions of the dispersion equations related to sensing applications are obtained. Sharma and Pathania [25] studied thermoelastic Lamb waves in a homogeneous isotropic plate bordered with layers of inviscid liquid in the context of coupled theory of thermoelasticity.

The piezothermoelastic material response entails an interaction of three major fields, namely, mechanical, thermal and electric in the macro-physical world. One of the applications of the piezothermoelastic material is to detect the responses of a structure by measuring the electric charge, sensing or to reduce excessive responses by applying additional electric forces or thermal forces, actuating. If sensing and actuating can be integrated smartly, a so-called intelligent structure can be designed. The piezoelectric materials are also often used as resonators whose frequencies need to be precisely controlled. Because of the coupling between the thermoelastic and pyroelectric effects, it is important to quantify the effect of heat dissipation on the propagation of wave at low and high frequencies. Yang and Batra [26] studied the effect of heat conduction on shift in the frequencies of a freely vibrating linear piezoelectric body with the help of two perturbation methods. It is shown that the first order effect on frequencies is to shift them by a small imaginary number, thereby signifying that the effect of energy dissipation due to heat conduction is to reduce the amplitude of vibration. Sharma and Kumar [27] have studied the propagation of plane harmonic waves in piezothermoelastic materials. No problem which analyses the propagation of Lamb-type waves in piezothermoelastic materials analytically is available in the literature as per the knowledge of authors.

In the present paper, an attempt has been made to investigate the propagation of Lamb waves in piezothermoelastic, transversely isotropic elastic plate that is subjected to stress- and charge-free, thermally insulated/isothermal boundary conditions. The Rayleigh Lamb-type dispersion relations have been obtained in both the cases, for symmetric and skew symmetric modes of wave propagation in the plate. The dilatation, electric potential and temperature change are also computed. The analytical results have been verified and computed numerically for

cadmium-selenide (Cd Se) material plate, which are found to be in close agreement with the analytical results.

2. Formulation of the problem

We consider an infinite homogeneous, transversely isotropic, piezothermoelastic plate of thickness '2d' initially at uniform temperature T_0 and electric potential ϕ_0. We take origin of the co-ordinate system (x_1, x_2, x_3) on the middle surface of the plate. The $x_1 - x_2$ plane is chosen to coincide with middle surface and x_3-axis normal to it along the thickness. The surfaces $x_3 = \pm d$ are subjected to different boundary conditions. We take $x_1 - x_3$ as the plane of incidence and assume that the solutions are explicitly independent of x_2 but implicit dependence is there, so that the component u_2 of displacement vector is non-vanishing. The basic governing equations for homogeneous transversely isotopic piezothermoelasticity, in the absence of charge density, heat sources and body forces, are given by

$$c_{11}u_{1,11} + c_{44}u_{1,13} + (c_{13} + c_{44})u_{3,13} + (e_{15} + e_{31})\phi_{,13} - \beta_1 T_{,1} = \rho\ddot{u}_1, \tag{1}$$

$$c_{66}u_{2,11} + c_{44}u_{2,33} = \rho\ddot{u}_2, \tag{2}$$

$$(c_{13} + c_{44})u_{1,13} + c_{44}u_{3,11} + c_{33}u_{3,33} + e_{15}\phi_{,11} + e_{33}\phi_{,33} - \beta_3 T_{,3} = \rho\ddot{u}_3, \tag{3}$$

$$(e_{15} + e_{31})u_{1,13} + e_{15}u_{3,11} + e_{33}u_{3,33} - \epsilon_{11}\phi_{,11} - \epsilon_{33}\phi_{,33} + p_3 T_{,3} = 0, \tag{4}$$

$$K_{11}T_{,11} + K_{33}T_{,33} - \rho C_e\dot{T} = T_0\left[\beta_1\dot{u}_{1,1} + \beta_3\dot{u}_{3,3} - p_3\dot{\phi}_{,3}\right], \tag{5}$$

where

$$\beta_1 = (c_{11} + c_{12})\alpha_1 + c_{13}\alpha_3, \quad \beta_3 = 2c_{13}\alpha_1 + c_{33}\alpha_3.$$

α_1, K_{11} are coefficients of linear thermal expansion and thermal conductivity, respectively, in the direction orthogonal to the axes of symmetry, α_3, K_3 the corresponding quantities along the axis of symmetry; ρ, C_e are, respectively, the density and specific heat at constant strain, c_{ij} are the isothermal elastic parameters, e_{ij} are the piezoelectric constants, ϵ_{11} and ϵ_{33} are electric permittivities and p_3 is pyroelectric constant. Here the superposed dot denotes time differentiation and coma notation is used for spatial derivatives. In Eqs. (1)–(5), $\vec{u} = (u_1, u_2, u_3)$ is the displacement vector, ϕ is the electric potential and $T(x_1, x_2, x_3, t)$ is the temperature change. Eqs. (1)–(5) can be written in non-dimensional form as

$$u_{1,11} + c_2u_{1,33} + c_3u_{3,13} + \epsilon_p e_1\phi_{,13} - T_{,1} = \ddot{u}_1, \tag{6}$$

$$c_2u_{2,33} + c_4u_{2,11} = \ddot{u}_2, \tag{7}$$

$$c_3u_{1,13} + c_2u_{3,11} + c_1u_{3,33} + \epsilon_p(e_2\phi_{,11} + \phi_{,33}) - \bar{\beta}T_{,3} = \ddot{u}_3, \tag{8}$$

$$e_1u_{1,13} + e_2u_{3,11} + u_{3,33} - \epsilon_\eta(\bar{\epsilon}\phi_{,11} + \phi_{,33}) + pT_{,3} = 0, \tag{9}$$

$$T_{,11} + \bar{K}T_{,33} - \dot{T} = \epsilon[\dot{u}_{1,1} + \bar{\beta}\dot{u}_{3,3} - \epsilon_p p\dot{\phi}_{,3}], \tag{10}$$

where we have defined the following quantities:

$$x_i' = \frac{\omega^* x_i}{v_P}, \quad t' = \omega^* t, \quad u_i' = \frac{\rho\omega^* v_p u_i}{\beta_1 T_0}, \quad T' = \frac{T}{T_0}, \quad \phi' = \frac{\phi}{\phi_0}, \quad \omega^* = \frac{C_e c_{11}}{K_{11}}, \quad \epsilon = \frac{T_0\beta_1^2}{\rho C_e c_{11}},$$

$$v_P = \sqrt{\frac{c_{11}}{\rho}}, \quad p = \frac{p_3 c_{11}}{\beta_1 e_{33}}, \quad c_1 = \frac{c_{33}}{c_{11}}, \quad c_2 = \frac{c_{44}}{c_{11}}, \quad c_3 = \frac{c_{13}+c_{44}}{c_{11}}, \quad c_4 = \frac{c_{11}-c_{12}}{2c_{11}},$$

$$e_1 = \frac{e_{15}+e_{31}}{e_{33}}, \quad e_2 = \frac{e_{15}}{e_{33}}, \quad \bar{\epsilon} = \frac{\epsilon_{11}}{\epsilon_{33}}, \quad \epsilon_P = \frac{\omega^* e_{33}\phi_0}{v_P\beta_1 T_0}, \quad \epsilon_\eta = \eta_3\epsilon_P,$$

$$\eta_3 = \frac{\epsilon_{33}c_{11}}{e_{33}^2}, \quad \omega' = \frac{\omega}{\omega^*}, \quad c' = \frac{c}{v_P}, \quad d' = \frac{\omega^* d}{v_P}, \quad h' = \frac{h v_P}{\omega^*},$$

$$\xi' = \frac{\xi v_P}{\omega^*}, \quad \sigma_{ij}' = \frac{\sigma_{ij}}{\beta_1 T_0}, \quad \bar{\beta} = \frac{\beta_3}{\beta_1}, \quad \bar{K} = \frac{K_{33}}{K_{11}}. \tag{11}$$

Here ϵ is the thermoelastic coupling constant, ω^* is the characteristic frequency of the medium, ϵ_p is the piezothermoelastic coupling constant and v_P is the longitudinal wave velocity in the medium. The primes have been suppressed for convenience.

2.1. Boundary conditions

The non-dimensional boundary conditions at the surfaces $x_3 = \pm d$ of the plate are given by

(i) *Mechanical conditions* (stress-free surfaces)

$$\sigma_{33} = 0, \quad \sigma_{13} = 0, \quad \sigma_{23} = 0. \tag{12.1}$$

(ii) *Thermal conditions*

$$T_{,3} + hT = 0, \tag{12.2}$$

where h is the surface heat transfer coefficient. Here $h \to 0$ corresponds to thermally insulated boundaries and $h \to \infty$ refers to isothermal surfaces.

(iii) *Electrical conditions* (charge free surfaces)

$$D_3 = 0 \tag{12.3}$$

for charge-free surfaces and where D_3 is the electrical displacement.

3. Solution of the problem

We assume solution of the form

$$(u_1, u_2, u_3, \phi, T) = (1, \bar{u}_2, V, W, S)U \exp[\mathrm{i}\xi(x_1 \sin\theta + m x_3 - ct)], \tag{13}$$

where ξ is the wave number, ω is the angular frequency and $c = \omega/\xi$ is the phase velocity of the wave. Here θ is the angle of inclination of wave normal with axes of symmetry (x_3-axis), m is still

an unknown parameter which signifies the penetration depth of the wave; $\bar{u}_2$, V, W and S are, respectively, the amplitude ratios of displacements u_2, u_3 electric potential ϕ and temperature T to that of displacement u_1. The use of Eq. (13) in Eqs. (6)–(10) leads to a system of the following coupled equations for the amplitudes $[1, V, W, S, \bar{u}_2]^{\mathrm{T}}$:

$$\begin{bmatrix} s^2+c_2m^2-c^2 & c_3ms & \epsilon_p e_1 ms & -s & 0 \\ c_3ms & c_2s^2+c_1m^2-c^2 & \epsilon_p(e_2s^2+m^2) & -\bar{\beta}m & 0 \\ e_1ms & e_2s^2+m^2 & -\epsilon_\eta(\bar{\epsilon}s^2+m^2) & pm & 0 \\ c^2\epsilon s & c^2\epsilon\bar{\beta}m & -c^2\epsilon\epsilon_p pm & c^2+z(s^2+\bar{K}m^2) & 0 \\ 0 & 0 & 0 & 0 & c_2m^2+c_4s^2-c^2 \end{bmatrix} \begin{bmatrix} 1 \\ V \\ W \\ S \\ \bar{u}_2 \end{bmatrix} = \begin{bmatrix} 0 \\ 0 \\ 0 \\ 0 \\ 0 \end{bmatrix}, \tag{14}$$

where $z = \mathrm{i}\omega$, $s = \sin\theta$. The system of Eq. (14) has a non-trivial solution if the determinant of coefficients of $[1, V, W, S, \bar{u}_2]^{\mathrm{T}}$ vanishes, which leads to the following polynomial characteristic equation:

$$m^8 + \left(a_1 + \frac{s^2}{\bar{K}} + \frac{Fc^2}{z\bar{K}}\right)m^6 + \left(a_2 + a_1\frac{s^2}{\bar{K}} + \frac{Fc^2}{\bar{K}z}A_1\right)m^4 + \left(a_3 + a_2\frac{s^2}{\bar{K}} + \frac{Fc^2}{\bar{K}z}A_2\right)m^2 + \left(a_3\frac{s^2}{\bar{K}} + \frac{Fc^2A_3}{\bar{K}z}\right) = 0, \tag{15}$$

$$c_2m^2 + c_4s^2 - c^2 = 0, \tag{16}$$

where the coefficients a_i and A_i, $i = 1, 2, 3$ are given in the appendix. Eq. (16) corresponds to purely transverse (SH) wave mode that decoupled from rest of the motion and is not effected by either of the thermal variations, pyroelectric or piezoelectric effects and hence will not be considered in the following analysis. Eq. (15) being a biquadratic in m^2 admits eight solutions for m which also have the property $m_2 = -m_1, m_4 = -m_3, m_6 = -m_5, m_8 = -m_7$.

For each m_q, $q = 1, 3, ..., 8$, the amplitude ratios V, W, and S can be expressed as

$$V_q = R_1(m_q)/R(m_q), \quad W_q = R_2(m_q)/R(m_q), \quad S_q = R_3(m_q)/R(m_q), \tag{17}$$

where $R(m_q)$ and $R_i(m_q)$, $i = 1, 2, 3$ are given in the appendix. Combining Eq. (17) with stress, strain, electric displacement and temperature relation given below,

$$\sigma_{33} = (c_3 - c_2)u_{1,1} + c_1u_{3,3} + \epsilon_P\phi_{,3} - \bar{\beta}T,$$

$$\sigma_{13} = c_2(u_{1,3} + u_{3,1}) + \epsilon_P e_2\phi_{,1}, \quad D_3 = (e_1 - e_2)u_{1,1} + u_{3,3} - \epsilon_\eta\phi_{,3} + pT, \tag{18}$$

we rewrite the formal solution for displacements, temperature and electric potential, as

$$(u_1, u_3, \phi, T) = \sum_{q=1}^{8} (1, V_q, W_q S_q) U_q \exp[\mathrm{i}\xi(x_1 \sin\theta + m x_3 - ct)]. \tag{19}$$

The stresses, electric displacement and temperature gradient are obtained as

$$(\sigma_{33}, \sigma_{13}, D_3, T_{,3}) = \sum_{q=1}^{8} \mathrm{i}\xi (D_{1q}, D_{2q}, D_{3q}, m_q S_q) U_q \mathrm{e}^{\mathrm{i}\xi(x_1 \sin\theta + x_3 m_q - ct)}, \tag{20}$$

where

$$D_{1q} = (c_3 - c_2)\sin\theta + c_1 m_q V_q + \epsilon_p m_q W_q - \frac{\bar{\beta}}{\mathrm{i}\xi} S_q, \tag{21.1}$$

$$D_{2q} = c_2 m_q + c_2 \sin\theta\, V_q + \epsilon_p e_2 \sin\theta\, W_q, \tag{21.2}$$

$$D_{3q} = (e_1 - e_2)\sin\theta + m_q V_q - \epsilon_\eta m_q W_q + \frac{p}{\mathrm{i}\xi} S_q, \quad q = 1, 2, 3, \ldots, 8. \tag{21.3}$$

4. Derivation of the secular equations

We consider two types of thermal boundary condition of the plate namely, isothermal boundaries and thermally insulated boundaries.

4.1. Stress- and charge-free, isothermal boundary conditions ($h \to \infty$)

By invoking stress-free, isothermal and electrically charge-free boundary conditions (12.1), (12.2) and (12.3) at the plate surfaces $x_3 = \pm d$, we obtain a system of eight simultaneous linear equations in amplitudes U_q, $q = 1, 2, \ldots, 8$ as

$$\sum_{q=1}^{8} D_{1q} E_q U_q = 0, \ \sum_{q=1}^{8} D_{2q} E_q U_q = 0, \ \sum_{q=1}^{8} D_{3q} E_q U_q = 0, \ \sum_{q=1}^{8} D_{4q} E_q U_q = 0, \tag{22}$$

where $D_{4q} = (m_q + h) S_q$ and $E_q = \mathrm{e}^{\pm \mathrm{i}\xi m_q d}$, $q = 1, 2, 3 \ldots 8$ system of Eqs. (22) have a non-trivial solution if the determinant of the coefficients of U_q, $q = 1, 2, \ldots, 8$ vanishes, which leads to a characteristic equation for the propagation of modified guided waves in the plate. The characteristic equation for the piezothermoelastic waves in this case after applying lengthy algebraic reductions and manipulations leads to the following secular equations:

$$\left[\frac{T_1}{T_5}\right]^{\pm 1} - \frac{D_{23} G_3}{D_{21} G_1}\left[\frac{T_3}{T_5}\right]^{\pm 1} - \frac{D_{27} G_7}{D_{21} G_1}\left[\frac{T_7}{T_5}\right]^{\pm 1} = \frac{-D_{25} G_5}{D_{21} G_1}, \tag{23}$$

where

$$T_1 = \tan(\gamma m_1), \quad T_3 = \tan(\gamma m_3), \quad T_5 = \tan(\gamma m_5), \quad T_7 = \tan(\gamma m_7), \quad \gamma = \xi d, \tag{24}$$

$$G_1 = \begin{vmatrix} D_{13} & D_{15} & D_{17} \\ D_{33} & D_{35} & D_{37} \\ D_{43} & D_{45} & D_{47} \end{vmatrix}, \quad G_3 = \begin{vmatrix} D_{11} & D_{15} & D_{17} \\ D_{31} & D_{35} & D_{37} \\ D_{41} & D_{45} & D_{47} \end{vmatrix}, \quad G_5 = \begin{vmatrix} D_{11} & D_{13} & D_{17} \\ D_{31} & D_{33} & D_{37} \\ D_{41} & D_{43} & D_{47} \end{vmatrix},$$
$$G_7 = \begin{vmatrix} D_{11} & D_{13} & D_{15} \\ D_{31} & D_{33} & D_{35} \\ D_{41} & D_{43} & D_{45} \end{vmatrix}. \tag{25}$$

Here $D_{4q} = S_q$ and D_{1q}, D_{2q}, D_{3q} are defined in Eqs. (21.1)–(21.3). In Eq. (23) the superscript -1 corresponds to symmetric and $+1$ refers to antisymmetric modes of wave propagation in the plate.

4.2. Stress and charge free, thermally insulated boundary conditions ($h \to 0$)

Upon invoking the stress-free, and electrically charge-free, thermally insulated boundary conditions (12.1), (12.2) and (12.3) at $x_3 = \pm d$, we obtain the secular equations

$$\frac{G_{57}}{G_{37}}\left[\frac{T_1 T_3}{T_5}\right]^{\pm 1} + \frac{G_{35}}{G_{37}}\left[\frac{T_1 T_7}{T_5}\right]^{\pm 1} + \frac{G_{15}}{G_{37}}\left[\frac{T_3 T_7}{T_5}\right]^{\pm 1} = -\left[T_1^{\pm 1} + \frac{G_{17}}{G_{37}} T_3^{\pm 1} + \frac{G_{13}}{G_{37}} T_7^{\pm 1}\right], \tag{26}$$

where

$$\begin{aligned} G_{13} &= (D_{11}D_{33} - D_{31}D_{13})(D_{25}D_{47} - D_{27}D_{45}), & G_{57} &= (D_{15}D_{37} - D_{35}D_{17})(D_{21}D_{43} - D_{23}D_{41}), \\ G_{15} &= (D_{11}D_{35} - D_{31}D_{15})(D_{27}D_{43} - D_{23}D_{47}), & G_{37} &= (D_{13}D_{37} - D_{33}D_{17})(D_{25}D_{41} - D_{21}D_{45}), \\ G_{17} &= (D_{11}D_{37} - D_{31}D_{17})(D_{23}D_{45} - D_{25}D_{43}), & G_{35} &= (D_{13}D_{35} - D_{33}D_{15})(D_{21}D_{47} - D_{27}D_{41}). \end{aligned} \tag{27}$$

Here $D_{4q} = m_q S_q$ and D_{1q}, D_{2q}, D_{3q} are defined in Eqs. (21.1)–(21.3).

Secular equations (23) and (26) are the transcendental equations which contain complete information about the phase velocity, wave number and attenuation coefficient of the plate waves. In general, wave number and hence the phase velocity of the waves is a complex quantity; therefore the waves are attenuated in space. If we write

$$c^{-1} = v^{-1} + \mathrm{i}\omega^{-1} q, \tag{28}$$

where v and q are real; the exponent in the plane wave solution (13) becomes

$$-q(x_1 \sin\theta + m x_3) - \mathrm{i}\omega\{v^{-1}(x_1 \sin\theta + m x_3) - t\}. \tag{29}$$

This shows that v is the propagation velocity and q is the attenuation coefficient of the wave. Upon using Eq. (28) in Eqs. (23) and (26), the values of v and q for different modes can be obtained.

5. Special cases

5.1. Uncoupled thermoelasticity (piezoelectricity)

If we set $\epsilon = 0 = p$, the motion corresponding to the thermal wave (T-mode) decouples from rest of the motion and the various results reduce to those of piezoelectric elastic plate. Secular equations (23) and (26) for symmetric and skew symmetric modes for rest of the motion under various boundary conditions take the following forms:

$$\left[\frac{T_1}{T_5}\right]^{\pm 1} - \frac{D'_{23}F_3}{D'_{21}F_1}\left[\frac{T_3}{T_5}\right]^{\pm 1} = -\frac{D'_{25}F_5}{D'_{21}F_1}, \tag{30}$$

$$F_1 = D'_{13}D'_{35} - D'_{33}D'_{15},\ F_3 = D'_{11}D'_{35} - D'_{31}D'_{15},\ F_5 = D'_{11}D'_{33} - D'_{31}D'_{13},$$

where

$$\begin{aligned} D'_{1q} &= (c_3 - c_2)\sin\theta + c_1 m_q V'_q + m_q W'_q, \\ D'_{2q} &= c_2 m_q + c_2 \sin\theta V'_q + e_2 \sin\theta W'_q, \\ D'_{3q} &= (e_1 - e_2)\sin\theta + m_q V'_q - \eta_3 m_q W'_q, \\ V'_q &= -R'_1(m_q)/R'(m_q), \quad W'_q = R'_2(m_q)/R'(m_q), \end{aligned} \tag{31}$$

$$\begin{aligned} R'_1(m_q) &= \left[c_2 e_3 m_q^4 + \left\{(e_3 + c_2 e_2 - e_1 c_3)s^2 - e_3 c^2\right\}m_q^2 + e_2 s^2(s^2 - c^2)\right], \\ R'_2(m_q) &= c_1 c_2 m_q^4 + (Ps^2 - Jc^2)m_q^2 + (s^2 - c^2)(c_2 s^2 - c^2), \\ R'(m_q) &= m_q s\left[(c_3 e_3 - c_1 e_1)m_q^2 + (c_3 e_2 - e_1 c_2)s^2 + e_1 c^2\right]. \end{aligned} \tag{32}$$

Here m_q, $q = 1, 2, 3, 4, 5, 6$, are the roots of the equation

$$m^6 + a_1 m^4 + a_2 m^2 + a_3 = 0, \tag{33}$$

where a_1, a_2, a_3 are defined in the appendix.

5.2. Thermoelastic plate

In the absence of piezoelectricity, we set $\epsilon_P = 0 = p$; the various results reduce to those of stress-free thermoelastic plate. The secular equations (23) and (26) for symmetric and skew symmetric modes for rest of the motion under various boundary conditions take the following forms:

$$\left[\frac{T_1}{T_5}\right]^{\pm 1} - \frac{D^*_{27}G^*_7}{D^*_{21}G^*_1}\left[\frac{T_3}{T_5}\right]^{\pm 1} = -\frac{D^*_{25}G^*_5}{D^*_{21}G^*_1}, \tag{34}$$

where

$$G^*_1 = D^*_{15}D^*_{47} - D^*_{17}D^*_{45}, \quad G^*_5 = D^*_{11}D^*_{47} - D^*_{17}D^*_{41}, \quad G^*_7 = D^*_{11}D^*_{45} - D^*_{15}D^*_{41},$$

$$\begin{aligned} D^*_{1q} &= (c_3 - c_2)\sin\theta + c_1 m_q V^*_q - \bar{\beta}S_q/\mathrm{i}\xi, \\ D^*_{2q} &= c_2 m_q + c_2 \sin\theta\, V^*_q, \end{aligned} \tag{35}$$

$$D_{4q}^{*}=\begin{cases} S_q^{*} & \text{for isothermal,}\\ m_q S_q^{*} & \text{for thermally insulated,}\end{cases}$$

$$V_q^{*}=\begin{cases} m_q\alpha_q/\sin\theta, & q=1,2,7,8,\\ -\sin\theta/m_q\alpha_q, & q=5,6,\end{cases}$$

$$S_q^{*}=\begin{cases} [(c_2+c_3\alpha_q)m_q^2+s^2-c^2]/s, & q=1,2,7,8,\\ [c_2m_q^2+(1-c_3/\alpha_q)s^2-c^2]/s, & q=5,6,\end{cases} \tag{36}$$

$$\alpha_q=\bar{\beta}\frac{[c_2m_q^2+(1-c_3/\bar{\beta})s^2-c^2]}{(c_1-c_3\bar{\beta})m_q^2+c_2s^2-c^2}.$$

Here m_q, $q=1,2,5,6,7,8$, are the roots of the equation obtained by equating to zero the determinant of Eq. (14) after ignoring the third and fifth rows and columns. Eq. (34) has been solved and discussed in detail by Sharma [28] for isotropic materials.

5.3. Stress-free elastic plate

In the absence of piezoelectric, pyroelectric and thermal effects, the secular equations (23) and (26) reduce to

$$\frac{T_1}{T_5}=\left[\frac{D_{15}''D_{21}''}{D_{11}''D_{25}''}\right]^{\pm 1}, \tag{37}$$

where $D_{1q}''=(c_3-c_2)\sin\theta+c_1m_qV_q''$, $D_{2q}''=c_2(m_q+\sin\theta\,V_q'')$, $q=1,5$,

$$V_q''=-\frac{c_3m_qs}{c_1m_q^2+c_2s^2-c^2}=-\frac{c_2m_q^2+s^2-c^2}{c_3m_qs},\quad q=1,5.$$

Here the roots m_1 and m_5 are given by

$$m_1^2+m_5^2=\frac{-(Ps^2-Jc^2)}{c_1c_2},\quad m_1^2m_5^2=\frac{(s^2-c^2)(c_2s^2-c^2)}{c_1c_2}.$$

6. Waves at short wavelength

Some information on the asymptotic behavior is obtainable by letting $\xi\to\infty$. If we take, $\xi>\omega/\sqrt{c_2}$, it follows that $\xi>\omega$ and $c<1$; then we replace m_1, m_3, m_5 and m_7 in the secular equations by $\mathrm{i}m_1'$, $\mathrm{i}m_3'$, $\mathrm{i}m_5'$ and $\mathrm{i}m_7'$, respectively. Hence for $\xi\to\infty$,

$$\frac{\tanh(\gamma m_1)}{\tanh(\gamma m_5)}\to 1,\quad \frac{\tanh(\gamma m_3)}{\tanh(\gamma m_5)}\to 1,\quad \frac{\tanh(\gamma m_7)}{\tanh(\gamma m_5)}\to 1,$$

so that the secular equations (23), (26), (30), (34) and (37), respectively, for both symmetric and antisymmetric cases reduce to

$$D_{21}G_1 - D_{23}G_3 + D_{25}G_5 - D_{27}G_7 = 0, \tag{38.1}$$

$$G_{13} + G_{15} + G_{17} + G_{35} + G_{37} + G_{57} = 0, \tag{38.2}$$

$$D'_{21}F_1 - D'_{23}F_3 + D'_{25}F_5 = 0, \tag{38.3}$$

$$D^*_{21}G^*_1 + D^*_{25}G^*_5 - D^*_{27}G^*_7 = 0, \tag{38.4}$$

$$D''_{11}D''_{25} - D''_{15}D''_{21} = 0. \tag{38.5}$$

Eqs. (38.1)–(38.5)) are merely Rayleigh surface wave equations in piezoelectric elasticity for stress- and charge-free, thermally insulated or isothermal surfaces of the plate and in elastokinetics, respectively. The Rayleigh results enter here since, for such small wavelengths, the finite thickness plate appears as a semi-infinite medium. Hence vibration energy is transmitted mainly along the surface of the plate.

7. Amplitudes of dilatation, temperature change and electric potential

The amplitudes of dilatation, electric potential and temperature during symmetric mode of vibration are obtained as

$$\begin{aligned} e &= \left(\frac{\partial u_1}{\partial x_1} + \frac{\partial u_3}{\partial x_3}\right) \\ &= \left[c'_1(\sin\theta + m_1 V_1) + Lc'_3(\sin\theta + m_3 V_3) + Mc'_5(\sin\theta + m_5 V_5) + Nc'_7(\sin\theta + m_7 V_7)\right] \\ &\quad \times A_1(\mathrm{i}\xi)\mathrm{e}^{\mathrm{i}\xi(x_1 \sin\theta - ct)}, \end{aligned} \tag{39.1}$$

$$\phi = \left[W_1 c'_1 + W_3 L c'_3 + W_5 M c'_5 + W_7 N c'_7\right] A_1(\mathrm{i}\xi)\mathrm{e}^{\mathrm{i}\xi(x_1 \sin\theta - ct)}, \tag{39.2}$$

$$T = \left[S_1 c'_1 + S_3 L c'_3 + S_5 M c'_5 + S_7 N c'_7\right] A_1(\mathrm{i}\xi)\mathrm{e}^{\mathrm{i}\xi(x_1 \sin\theta - ct)}, \tag{39.3}$$

where L, M, and N are given below.

$$\begin{aligned} L &= \left[D_{11}c^*_1(D_{25}D_{37}s^*_5c^*_7 - D_{35}D_{27}c^*_5s^*_7) - D_{15}c^*_5(D_{21}D_{37}s^*_1c^*_7 - D_{31}D_{27}c^*_1s^*_7)\right. \\ &\quad \left. + D_{17}c^*_7(D_{21}D_{35}s^*_1c^*_5 - D_{31}D_{25}c^*_1s^*_5)\right]/\Delta, \\ M &= \left[D_{13}c^*_3(D_{21}D_{37}s^*_1c^*_7 - D_{31}D_{27}c^*_1s^*_7) - D_{11}c^*_1(D_{23}D_{37}s^*_3c^*_7 - D_{33}D_{27}c^*_3s^*_7)\right. \\ &\quad \left. + D_{17}c^*_7(D_{23}D_{31}s^*_3c^*_1 - D_{33}D_{21}c^*_3s^*_1)\right]/\Delta, \\ N &= \left[D_{13}c^*_3(D_{25}D_{31}s^*_5c^*_1 - D_{35}D_{21}c^*_5s^*_1) - D_{15}c^*_5(D_{23}D_{31}s^*_3c^*_1 - D_{33}D_{21}c^*_3s^*_1)\right. \\ &\quad \left. + D_{11}c^*_1(D_{23}D_{35}s^*_3c^*_5 - D_{33}D_{25}c^*_3s^*_5)\right]/\Delta, \\ \Delta &= -\left[D_{13}c^*_3(D_{25}D_{37}s^*_5c^*_7 - D_{35}D_{27}c^*_5s^*_7) - D_{15}c^*_5(D_{23}D_{37}s^*_3c^*_7 - D_{33}D_{27}c^*_3s^*_7)\right. \\ &\quad \left. + D_{17}c^*_7(D_{23}D_{35}s^*_3c^*_5 - D_{33}D_{25}c^*_3s^*_5)\right], \\ c^*_q &= \cos\xi m_q d, \quad s^*_q = \sin\xi m_q d, \quad c'_q = \cos\xi m_q x_3, \quad s'_q = \sin\xi m_q x_3, \quad q = 1, 2, 3, \ldots, 8. \end{aligned}$$

The amplitudes of dilatation, electric potential and temperature change for antisymmetric mode of vibration are obtained from Eqs. (39.1)–(39.3) by interchanging c'_q with s'_q and L, M, N with L', M', N', respectively, where L', M', N' are obtained from L, M, N by replacing c^*_q with s^*_q.

8. Numerical results and discussion

The material chosen for the purpose of numerical calculations is (6 mm class) cadmium selenide (CdSe) of hexagonal symmetry, which is transversely isotropic material. The physical data for a single crystal of CdSe material is given as

$$c_{11} = 7.41 \times 10^{10}\,\mathrm{N\,m^{-2}},\quad c_{12} = 4.52 \times 10^{10}\,\mathrm{N\,m^{-2}},\quad c_{13} = 3.93 \times 10^{10}\,\mathrm{N\,m^{-2}},$$
$$c_{33} = 8.36 \times 10^{10}\,\mathrm{N\,m^{-2}},\quad c_{44} = 1.32 \times 10^{10}\,\mathrm{N\,m^{-2}},\quad \beta_1 = 0.621 \times 10^{6}\,\mathrm{N\,K^{-1}\,m^{-2}},$$
$$\beta_3 = 0.551 \times 10^{6}\,\mathrm{N\,K^{-1}\,m^{-2}},\quad e_{13} = -0.160\,\mathrm{C\,m^{-2}},\quad e_{33} = 0.347\,\mathrm{Cm^{-2}},$$
$$e_{51} = -0.138\,\mathrm{C\,m^{-2}},\quad \epsilon_{11} = 8.26 \times 10^{-11}\,\mathrm{C^2\,N^{-1}\,m^{-2}},\quad \epsilon_{33} = 9.03 \times 10^{-11}\,\mathrm{C^2\,N^{-1}\,m^{-2}},$$
$$C_e = 260\,\mathrm{J\,kg^{-1}K^{-1}},\quad p_3 = -2.94 \times 10^{-6}\,\mathrm{C\,K^{-1}m^{-2}},\quad Y_r = 4.48 \times 10^{10}\,\mathrm{N\,m^{-2}},$$
$$\alpha_r = 4.4 \times 10^{-6}\,\mathrm{K^{-1}},\quad \alpha_1 = 3.92 \times 10^{-12}\,\mathrm{C\,N^{-1}},\quad K_1 = K_3 = 9\,\mathrm{W\,m^{-1}\,K^{-1}},$$
$$\rho = 5504\,\mathrm{kg\,m^{-3}},\quad T_0 = 298\,\mathrm{K},\quad \omega^* = 2.14 \times 10^{13}\,\mathrm{s^{-1}}.$$

The secular equations (23) and (26) are solved numerically by the iteration method to obtain the phase velocity of symmetric and antisymmetric modes of vibrations after finding the roots m_i, $i = 1, 2, 3, \ldots, 8$ of the biquadratic equation (15) by using Descartes' method. In general, Eq. (15) is of the form $G(m, s, c) = 0$. Eq. (15) can be solved for 'm' by Descartes method for fixed values of c and s. The secular equations (23) and (26) are transcendental equations of the form $F(c, m) = 0$. For known values of m, this equation can also be solved for the phase velocity c. We have used iteration method to find the phase velocity for different values of wave number ξ and the procedure adopted is outlined below.

The iteration method to solve a transcendental equation $f(c) = 0$, requires to put this equation into the form $c = g(c)$, so that the sequence $\{c_n\}$ of iteration for the desired root can be easily generated as follows: If c_0 be the initial approximation to the root, then we have $c_1 = g(c_0), c_2 = g(c_1)$, $c_3 = g(c_3)$ and so on. In general, $c_{n+1} = g(c_n)$, $n = 0, 1, 2, 3, \ldots$. If $|g'(c)| \ll 1$, for all $c \in I$, then the sequence $\{c_n\}$ of approximations to the root will converge to the actual value $c = \zeta$ of the root, provided $c_0 \in I$, I being the interval in which root is expected. For initial value of $c = c_0 \in I$ and along direction 'θ', Eq. (15) can be solved for m by Descartes' method for a particular value of the non-dimensional wave number ξd. The values of m are then used in the secular equation to obtain a current value of c, which is further used to generate a new approximation to c. This process is repeated time and again for a particular value of the wave number ξd, unless the sequence of iterated approximations to the value of c converges to desired level of accuracy, i.e., $|c_{n+1} - c_n| < \varepsilon$, ε being an arbitrary small number to be selected at random in order to achieve the accuracy level. This procedure is continuously repeated for different values of the non-dimensional wave number ξd to obtain the phase velocity. Here, the sequence of the values of phase velocity has been allowed to iterate approximately for 100 iterations to make it converge in order to achieve the desired level of accuracy, viz. four decimal places. An infinite number of roots

exist for a given value of frequency, which can be obtained by giving a value of wave number, from the secular equations (23) and (26). Each root represents a propagating mode. Note that care must be taken in the root-finding procedure, for the transcendental functions change their values rapidly. The phase velocity ($v/\sqrt{c_2}$) profiles of the first three symmetric and antisymmetric modes of vibrations have been computed for various values of the non-dimensional wave number (ξd) from dispersion relations (23) and (26) in case of charge-free, thermally insulated/isothermal, stress-free plate of CdSe material. The corresponding dispersion curves and attenuation coefficient profiles for Rayleigh–Lamb-type modes are presented in Figs. 1–8, respectively. The amplitudes of dilatation, temperature and electric potential change in the case of fundamental mode have also been computed for charge- and stress-free isothermal plate in various directions ($\theta = 30^0, 45^0, 60^0, 75^0$) of propagation. These quantities are plotted with plate thickness in Figs. 9–14.

From Figs. 1 and 2, the velocity profiles of fundamental symmetric and skew symmetric modes for $\theta = 75^\circ$ in both isothermal and thermally insulated plates are noticed to be almost straight lines, indicating that these are nearly non-dispersive along this direction of propagation. All the modes show dispersive behavior in other considered directions of wave propagation. It is also seen that there are crossover points between various curves corresponding to the same mode in different directions of propagation. The crossover phenomenon physically indicates that at a particular wavelength, the mechanical/thermal/electrical energy may be exchangeable between the corresponding directions of wave propagation in the same mode. However, unlike elastic, thermoelastic and piezoelectric plate cases where the symmetric and skew symmetric modes are clearly distinguishable, it is no longer possible to very clearly define the symmetric and skew symmetric modes in a piezothermoelastic plate. It can be seen that as the wave number increases, the phase velocity of each mode decreases in all the directions of wave propagation. When wave

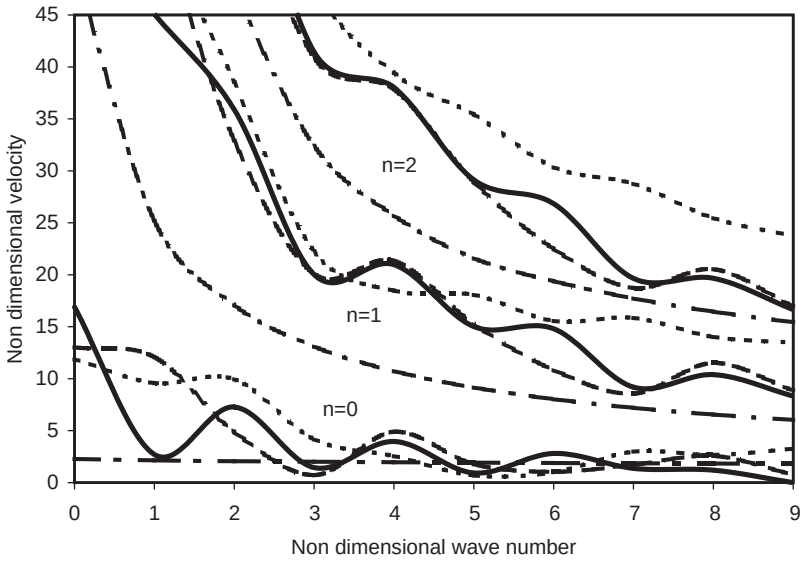

Fig. 1. Variation of non-dimensional phase velocity of symmetric modes of wave propagation with non-dimensional wave number in various directions (piezoelectric isothermal plate).

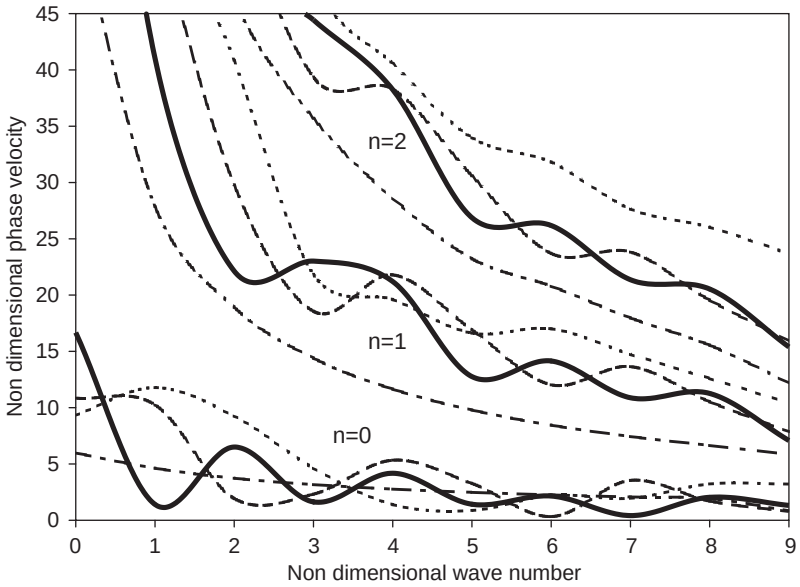

Fig. 2. Variation of non-dimensional phase velocity of skew symmetric modes of wave propagation with non-dimensional wave number in various directions (piezoelectric isothermal plate).

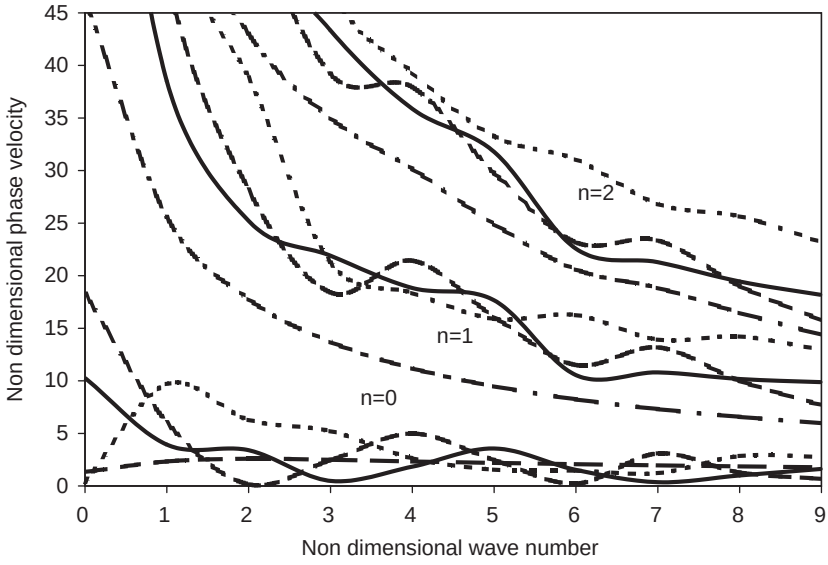

Fig. 3. Variation of non-dimensional phase velocity of symmetric modes of wave propagation with non-dimensional wave number in various directions (piezoelectric thermally insulated plate).

number becomes indefinitely large, the curves asymptotically approach to the Rayleigh wave velocity, because in such a situation a finite thickness plate behaves like a half-space and the transportation of energy takes place mainly across the free surface of the plate. For the low wave number, it is noticed that the phase velocity of the lowest mode in piezothermoelastic plate follows

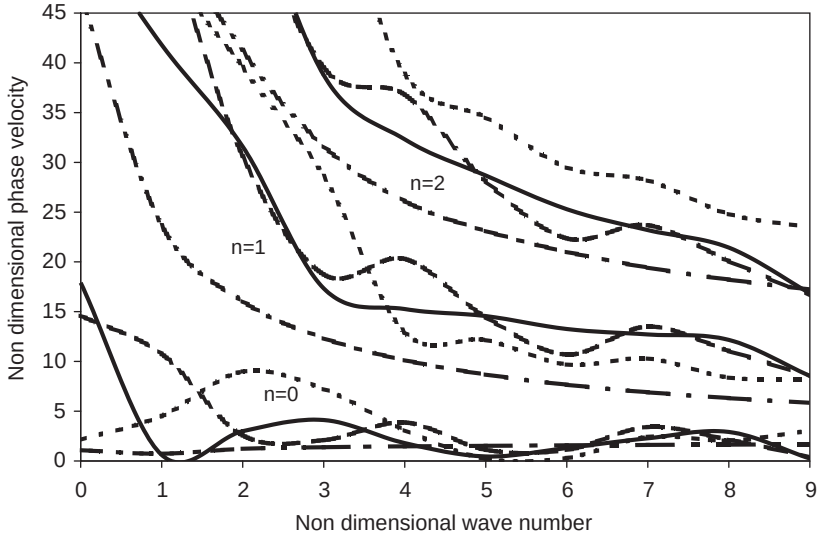

Fig. 4. Variation of non-dimensional phase velocity of skew symmetric modes of wave propagation with non-dimensional wave number in various directions (piezoelectric thermally insulated plate).

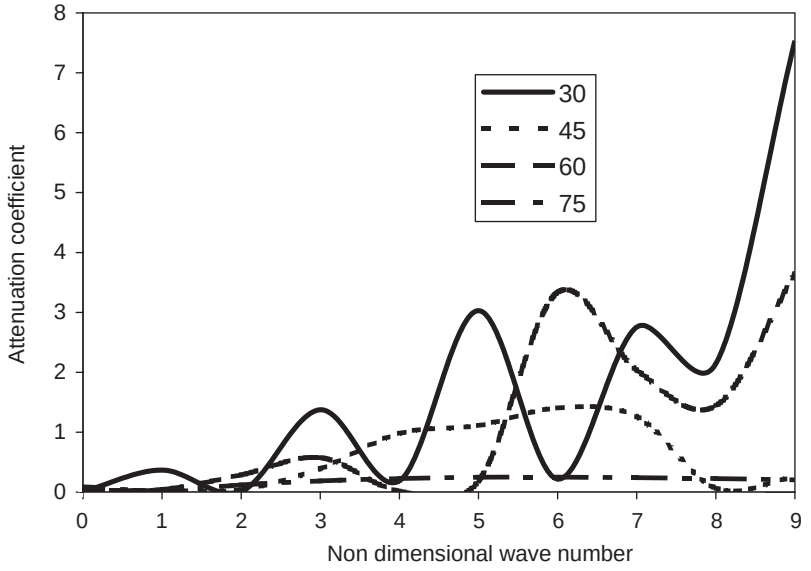

Fig. 5. Variation of attenuation coefficient of symmetric mode of wave propagation with non-dimensional wave number in various directions (piezoelectric isothermal plate).

closely that of the rotational wave speed of CdSe material. Except the fundamental mode, all higher modes have phase velocities greater than the shear wave speed in the considered range of wave number along all the directions of wave propagation. It is also observed that as the thickness of the piezothermoelastic plate increases, the phase velocity decreases in all the directions of wave propagation. This can be explained by the fact that as the thickness of the plate increases, the

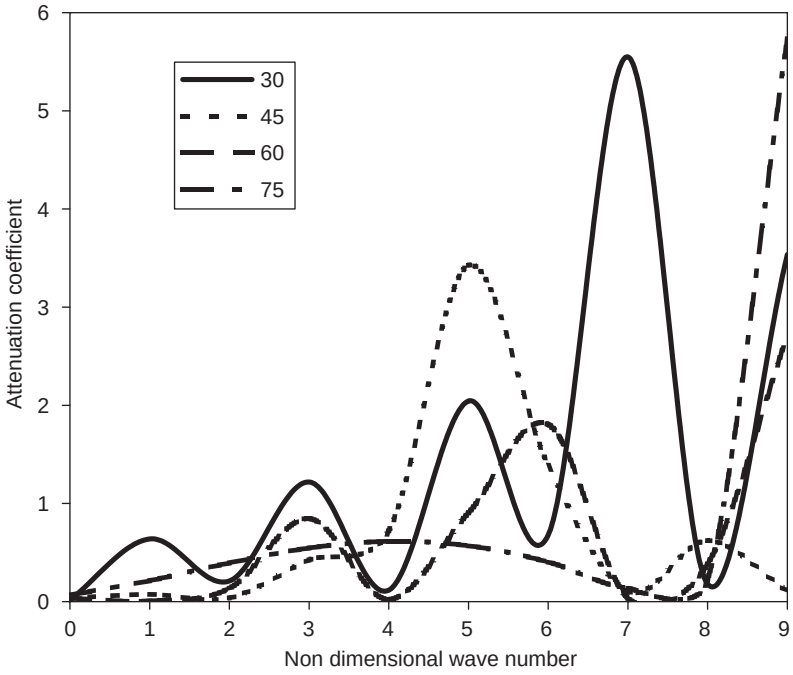

Fig. 6. Variation of attenuation coefficient of skew symmetric mode of wave propagation with non-dimensional wave number in various directions (piezoelectric isothermal plate).

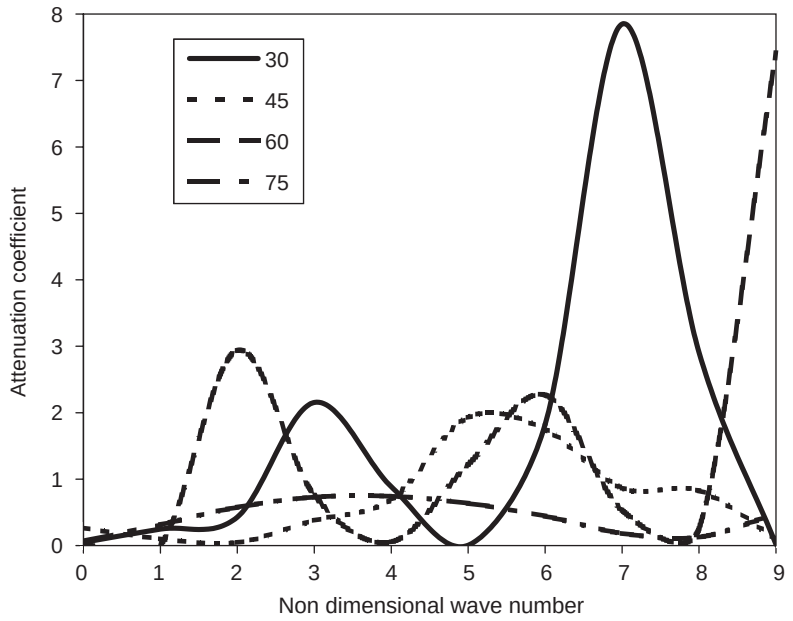

Fig. 7. Variation of attenuation coefficient of symmetric mode of wave propagation with non-dimensional wave number in various directions (piezoelectric thermally insulated plate).

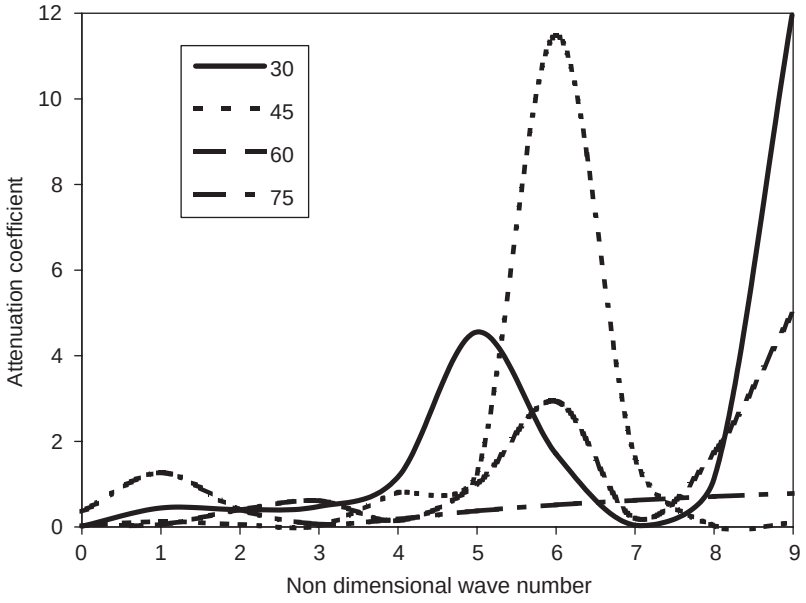

Fig. 8. Variation of attenuation coefficient of skew symmetric mode of wave propagation with non-dimensional wave number in various directions (piezoelectric thermally insulated plate).

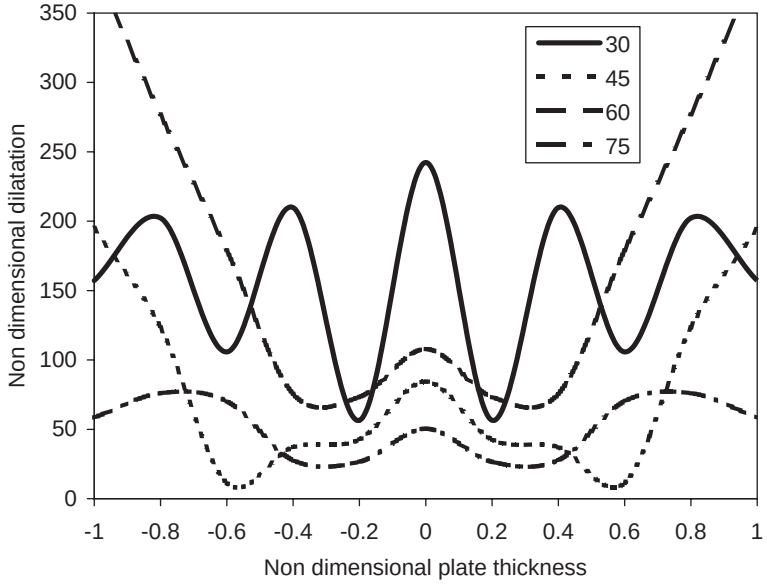

Fig. 9. Variation of symmetric dilatation with plate thickness in various directions.

coupling effect of various interacting fields also increases resulting in lower phase velocity. It can also be observed that the Rayleigh wave velocity is reached at a lower wave number as the thickness increases, because the transportation of energy mainly takes place in the neighbourhood of the free surfaces of the plate in this case. From Figs. 3 and 4 for $\theta = 75^\circ$, it is noticed that there

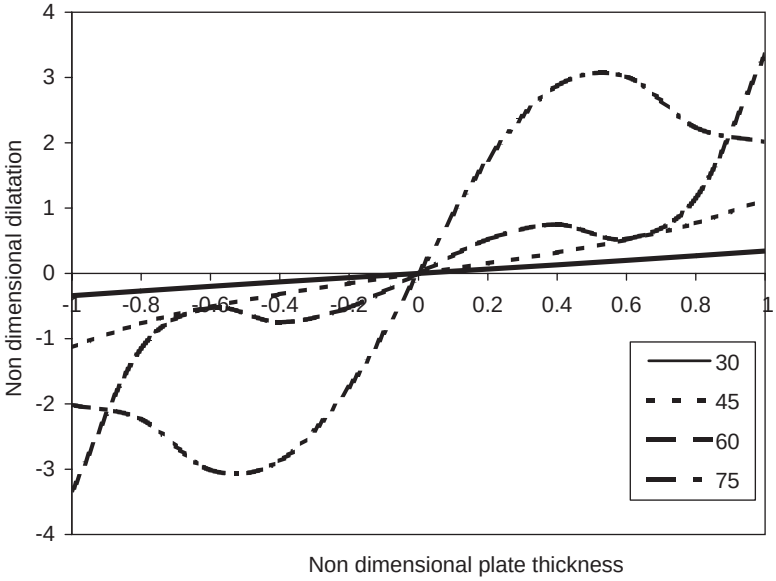

Fig. 10. Variation of skew symmetric dilatation with plate thickness in various directions.

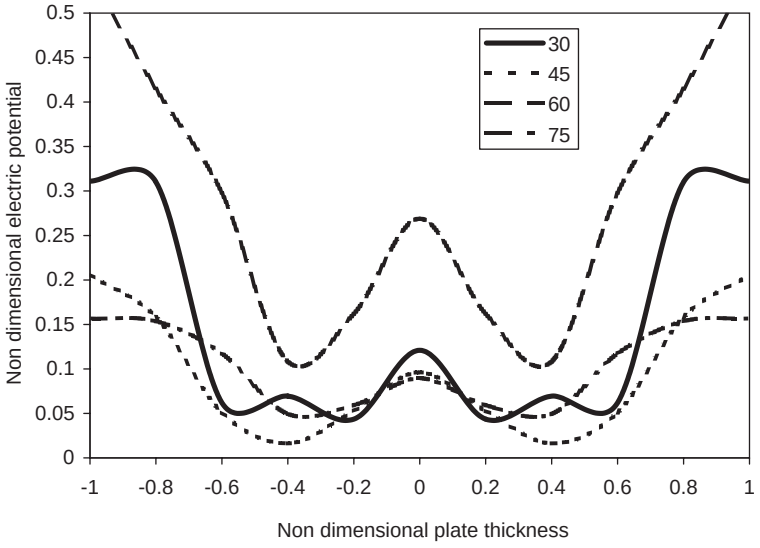

Fig. 11. Variation of amplitude of symmetric electric potential with plate thickness in various directions.

is almost negligible change in the behavior of fundamental (acoustical) and higher (optical) modes of propagation to that seen from Figs. 1 and 2 in this direction of propagation. Although significant changes and shifts are observed in the mode shapes along the other considered directions of propagation, the most effected velocity profiles are the one along $\theta = 30^\circ$ and $\theta = 45^\circ$ in this case. Thus, the effect of isothermal and thermally insulated boundaries of plate is also observed to be significant in CdSe material. The presence of dips in various curves shows the existence of damping phenomenon, which is noticed to be more prominent for $0 < \theta \leqslant 45^\circ$ than for

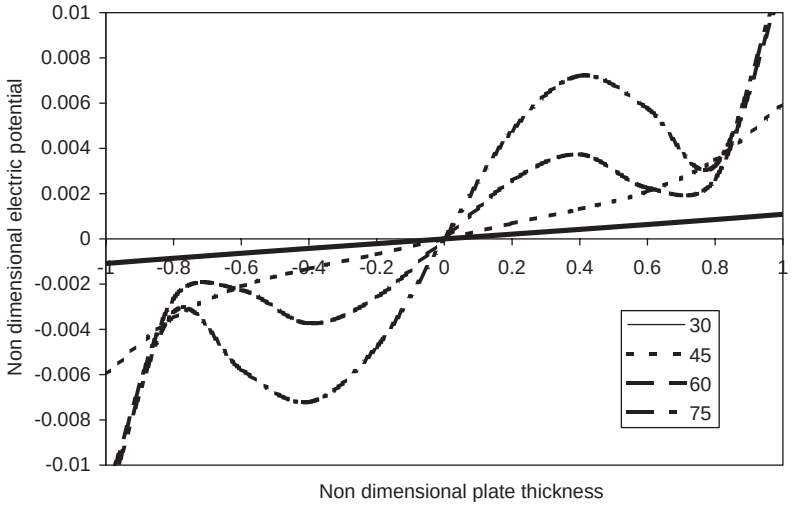

Fig. 12. Variation of amplitude of skew symmetric electric potential with plate thickness in various directions.

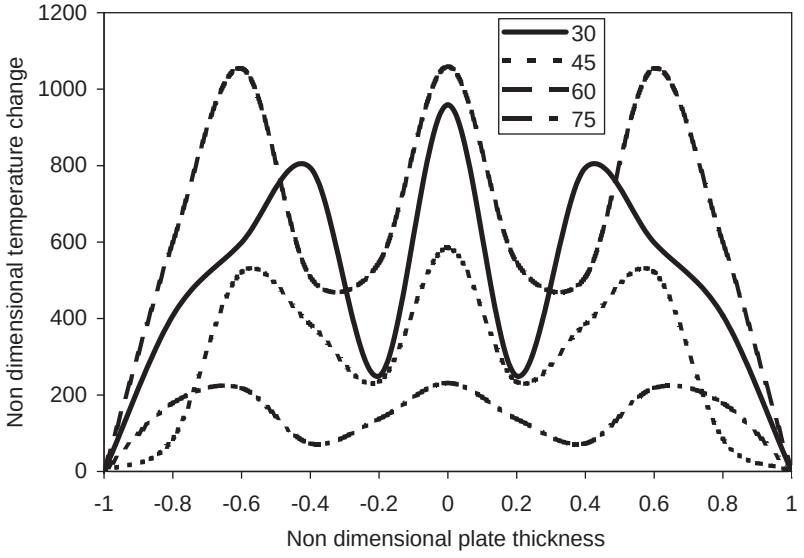

Fig. 13. Variation of amplitude of symmetric temperature change with plate thickness in various directions.

$45^\circ \leqslant \theta < 90^\circ$. However, the damping effect is quite significant along the directions for which θ satisfies the inequalities $30^\circ \leqslant \theta \leqslant 45^\circ$. No such dips are noticed to be present in the phase velocity profiles of fundamental (acoustical) and higher (optical) modes along $\theta = 75^\circ$ in both the cases of stress-free isothermal and stress-free thermally insulated, charge-free plate surfaces. Thus, the various modes of wave propagation are monotonic though attenuated/damped along this direction of wave propagation. Also, these dips are not observed in any of the curves for various modes in piezoelectric plate in the absence of thermal and pyroelectric effects. The oscillatory

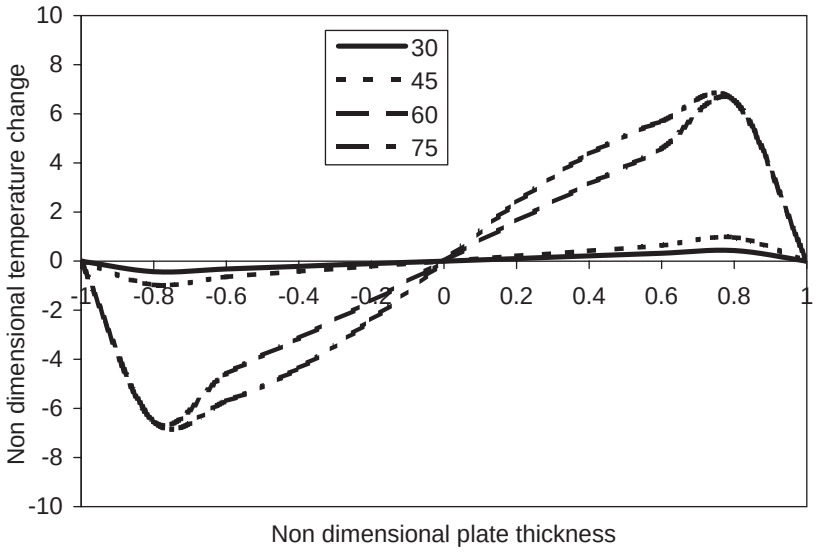

Fig. 14. Variation of amplitude of skew symmetric temperature change with plate thickness in various directions.

behavior is also not observed for thermoelastic plate in the absence of piezoelectric and pyroelectric effects. Clearly, the presence of these dips in various dispersion curves for the piezothermoelastic plate is attributed due to the coupling between thermal and electric fields, i.e. pyroelectric effects. The reduction in the amplitude of vibrations as compared to that of elastic and piezoelectric plate signifies the impact of energy dissipation due to heat conduction and pyroelectric effects.

The free surfaces admit a Rayleigh-type surface wave with complex wave number and hence phase velocity. Consequently, the surface wave propagates with attenuation due to the radiation of energy into the medium. This radiated energy will be reflected back to the center of the plate by the lower and upper surfaces. Consequently, the attenuated surface wave on the free surface is enhanced by this reflected energy to form a propagation wave. In fact, the multiple reflections between the upper and lower surfaces of the plate form caustics at one of the free surface and a strong stress concentration arises, due to which the wave field becomes unbounded in the limit $d \to \infty$. The unbounded displacement field is characterized by the singularities of circular tangent functions. Figs. 5 and 6 represent the variation of non-dimensional attenuation coefficient (q) of the waves with non-dimensional wave number (ξd) for acoustic mode of wave propagation in different directions in a plate with charge- and stress-free, isothermal surfaces. The amplitude of attenuation coefficient passes through many sign reversals through the thickness of the plate. The number of such sign reversals is quite high for $30^\circ \leqslant \theta \leqslant 60^\circ$ as compared to other directions of wave propagation. Therefore, the damping effect is more prominent in the considered range of wave number (ξd) along the direction of propagation for $30^\circ \leqslant \theta \leqslant 60^\circ$. From Fig. 6, it is noticed that attenuation coefficient for skew symmetric mode has quadratic variation at low wave number ($0 \leqslant \xi d \leqslant 8$) and then starts oscillating with quite high amplitude along $\theta = 75^\circ$. This quantity performs oscillations with increasing amplitude along other directions of wave propagation for the considered values of non-dimensional wave number. For the direction $\theta = 45^\circ$, the amplitude

of attenuation is observed to be quite high for the wave number range $4 \leqslant \xi d \leqslant 7$ with decreasing trend on either side of this interval. The variation of attenuation coefficient with wave number for thermally insulated plate during symmetric mode of wave propagation is similar to that of skew symmetric mode in isothermal plate except slight change in magnitude, which is clear from Figs. 6 and 7. Fig. 8 represents the attenuation coefficient profile of skew symmetric mode for a thermally insulated plate. The attenuation curve for $\theta = 75^\circ$ is almost a straight line indicating that in this direction attenuation coefficient is non-dispersive in character. In the direction $\theta = 45^\circ$, the magnitude of attenuation coefficient is very large in magnitude in the wave number range $5 \leqslant \xi d \leqslant 7$ and negligibly small on either side of this interval. This quantity observes oscillating behavior with increasing amplitude in other considered directions ($\theta = 30^\circ, 60^\circ$). Thus, the acoustic mode is noticed to be significantly attenuated in space and damped with time for both cases of charge- and stress-free, isothermal/thermally insulated plate surfaces along $\theta = 30^\circ$, 45° and 60°. Along the direction of propagation $\theta = 75^\circ$, the acoustic mode is free from peaks and dips and hence there is less damping effect. This result agrees with the corresponding result obtained earlier from the phase velocity profiles.

The amplitude of dilatation for fundamental symmetric and skew symmetric modes in an isothermal plate with respect to thickness in various directions of wave propagation is represented in Figs. 9 and 10, respectively. It is seen from Fig. 9 that there is large amplitude of symmetric dilatation near the upper and lower surfaces of the plate in all directions except for $\theta = 30^\circ$, which is primarily due to the presence of free surfaces because the upper and lower free surfaces give rise to the caustic effect which results in large-displacement amplitude and consequently to volumetric deformation (dilatation). Along $\theta = 30^\circ$ this quantity performs damped oscillations with maximum amplitude at the center of the plate. For a relatively thicker plate, the caustic effect becomes less important and the fundamental mode becomes a Rayleigh-type surface wave on the upper or lower free surface. In this case, one may still call the fundamental mode a Rayleigh-type surface wave on the free surface, for its amplitude on the free surface is several times of that elsewhere inside the plate. It is observed from Fig. 10 that there is maximum skew symmetric dilatation at the upper and lower surfaces of the plate and less deformation takes place at the center of the plate in all the directions of wave propagation. However, along the directions $\theta = 30^\circ$ and 45°, there is negligible variation in skew symmetric dilatation with plate thickness. The comparison of Figs. 9 and 10 reveals that the symmetric dilatation is noticed to be more dominant than the skew symmetric one, in this case.

The electric potential change along the plate thickness for fundamental symmetric and skew symmetric mode is plotted in Figs. 11 and 12. It is evident from Fig. 11 that maximum electric potential change is noticed at the upper and lower surfaces of the plate. Inside the plate electric potential change is very small and fluctuating. The variation of amplitude of electric potential during skew symmetric mode of vibration with plate thickness is shown in Fig. 12 for charge- and stress-free isothermal surfaces of the plate. Along $\theta = 30^0$ and 45°, the variation is almost linear with zero value at the center of the plate. But along the directions $\theta = 60^\circ$ and 75°, the absolute value of skew symmetric electric potential increases in $0 < x_3 < 0.4$ and decreases for $0.4 < x_3 < 0.7$ before it attains maximum value at the plate surfaces after a sharp increase. The symmetric electrical potential change is observed to be quite dominant and hence significant amount of mechanical and thermal energy gets converted into electrical energy during the propagation of mechanical or thermal disturbance in the present situation.

The symmetric temperature change with plate thickness is shown in Fig. 13 for isothermal boundaries of the plate. No temperature change is noticed at lower and upper surfaces of the plate, which is consistent with the boundary conditions. The symmetric temperature change is observed to behave like a damped oscillator on either side from the center of the plate where its amplitude is maximum. Moreover, the damping effect is quit high along the direction $\theta = 30^\circ$, 60°, moderate for $\theta = 45^\circ$ and observed to be least along $\theta = 75^\circ$. Thus, the effect of heat dissipation has less effect on wave propagation along the direction $\theta = 75^\circ$ than in other directions of wave propagation in the instant case. Fig. 14 represents the antisymmetric temperature change with plate thickness in a charge- and stress-free isothermal plate. The skew symmetric temperature change is zero at the center of the plate and also at the plate surfaces. The latter is consistent with boundary condition. The skew symmetric temperature change is noticed to be negligibly small, which varies almost linearly along the directions $\theta = 30^\circ$ and 45°, thereby establishing that this quantity is almost non-dispersive in character in these directions. Along $\theta = 60^\circ$ and 75°, the absolute value of skew symmetric temperature change increases monotonically for $|x| \leqslant 0.8$ and decreases for $|x| > 0.8$. From Figs. 13 and 14, it is clear that symmetric temperature change is more significant than the skew symmetric one in the present case. The velocity profile along the direction $\theta = 75^\circ$ is monotonically decreasing without peaks and dips, which is due to coupling between thermal and electric fields. Also, along this direction, there is minimum effect of pyroelectric fields as can be seen from the curves for dominant symmetric temperature and electric potential change in this direction.

9. Conclusions

Secular equations for symmetric and skew symmetric modes of vibration for piezothermoelastic Lamb waves in a plate have been derived for different boundary conditions. It is found that purely transverse (SH) wave decoupled from the rest of the motion and remains independent of piezoelectric, pyroelectric and thermal effects. From the dispersion curves, it is observed that decrease in phase velocity with wave number is oscillatory except along the direction $\theta = 75^\circ$. The acoustic mode of wave propagation is observed to be almost non-dispersive along the direction $\theta = 75^\circ$ of wave propagation. In all other directions, the decrease in velocity performs damped oscillations, which die out with increase in wave number. The lowest mode (acoustic mode) is most fluctuating. The oscillatory behavior of phase velocity with wave number seems to disappear with growing order of modes. This damping effect is not observed in thermoelastic and piezoelectric elastic plates, although the phase velocity ($v/\sqrt{c_2}$) profiles are attenuated. At short wavelength limits, the velocity of symmetric and antisymmetric modes of vibration asymptotically approaches the Rayleigh wave velocity. The attenuation coefficient profiles are found to increase with oscillating magnitude with wave number and have a number of peaks and dips. This establishes the effect of damping due to heat dissipation because of coupling between thermal and electric fields, viz. pyroelectric effects. But no such peaks and dips are observed in the velocity profile along the direction $\theta = 75^\circ$. This indicates that along this direction there is minimum effect of pyroelectric fields, as can also be seen from the curves for dominant symmetric temperature and electric potential change in this direction. The crossover points between various curves corresponding to same mode of propagation in different directions physically indicate that at a

particular wavelength, the mechanical/thermal/electrical energy may be exchangeable between the corresponding directions of wave propagation in the same mode. Unlike elastic, thermoelastic and piezoelectric elastic plate cases, the symmetric and skew symmetric modes in a piezothermoelastic plate are not very clearly distinguishable and the presence of peaks and dips is observed in various dispersion curves and attenuation profiles. This happens because of the pyroelectric effect as such as a phenomenon is not noticed in the absence of these effects in elastic, thermoelastic and piezoelectric plates. It is also observed that as the thickness of the piezothermoelastic plate increases, the phase velocity decreases in all the directions of propagation, because with increase in thickness of the plate, the coupling effect of various interacting fields also increases, resulting in lower phase velocity. It is also noticed that the Rayleigh wave velocity is reached at a lower wave number as the thickness increases, because the transportation of energy mainly takes place in the neighbourhood of the free surfaces of the plate in the considered case. The amplitudes of dilatation, electric potential and temperature change have also been computed and are shown graphically. The symmetric dilation, electric potential and temperature change are found to be more dominant than skew symmetric one in cadmium-selemide material plate. The dilatation is found to be maximum at the surfaces as compared to the center of the plate except along $\theta = 30^\circ$. This is primarily due to the presence of free surfaces which give rise to caustic effect. The electric potential is noticed to be maximum at the surfaces of the plate, which is physically relevant. The temperature change in the case of stress- and charge-free isothermal plate is found to be zero at the surfaces of the plate and the damping effect due to pyroelectric effect is found to be quite high along $\theta = 30^\circ$, 60°, moderate along $\theta = 45^\circ$ and least for $\theta = 75^\circ$, from the temperature change profile.

Acknowledgements

The authors thankfully acknowledge the financial support from the Council of Scientific and Industrial Research (CSIR), New Delhi, via project grants No. 25 (0115)/01/EMR-II.

Appendix A

The coefficients a_i, A_i, $i = 1, 2, 3$, in Eq. (15) and $R(m_q)$, $R_i(m_q)$, $i = 1, 2, 3$ in Eq. (17) are given as

$$a_1 = \frac{Ps^2 - Jc^2 + \bar{\epsilon}c_1c_2s^2 + \bar{\epsilon}_\eta\left[(2c_2e_2 - 2c_3e_1 + e_1^2c_1 + 1)s^2 - c^2\right]}{c_1c_2 + \bar{\epsilon}_\eta c_2},$$

$$a_2 = \frac{\bar{\epsilon}(Ps^2 - Jc^2) + (s^2 - c^2)(c_2s^2 - c^2) + \bar{\epsilon}_\eta[(e_1^2c_2 + e_2^2c_2 - 2c_3e_1e_2)s^4 - e_1^2s^2c^2 + 2e_2s^2(s^2 - c^2)]}{c_1c_2 + \bar{\epsilon}_\eta c_2},$$

$$a_3 = \frac{s^2(s^2 - c^2)\left[\bar{\epsilon}(c_2s^2 - c^2) + \bar{\epsilon}_\eta e_2^2s^2\right]}{c_1c_2 + \bar{\epsilon}_\eta c_2},$$

$$A_1 = \frac{\{E_1(P's^2 - J'\bar{c}^2) + \bar{\bar{\epsilon}}C_1C_2s^2 + \bar{\epsilon}_\eta[(2C_2\bar{e}_2 - (E+1)\bar{e}_1C_3 + \bar{e}_1^2C_1 + E^2)s^2 - E^2\bar{c}^2]\}}{C_1C_2E_1 + \bar{\epsilon}_\eta E^2C_2},$$

$$A_2 = \frac{\{\bar{\bar{\epsilon}}s^2(P's^2 - J'\bar{c}^2) + E_1(s^2 - \bar{c}^2)(C_2s^2 - \bar{c}^2) + \bar{\epsilon}_\eta[(\bar{e}_1^2C_2 + \bar{e}_2^2C_2 - 2C_3\bar{e}_1\bar{e}_2)s^4 + 2E\bar{e}_2(s^2 - \bar{c}^2)s^2 - \bar{e}_1^2s^2\bar{c}^2]\}}{C_1C_2E_1 + \bar{\epsilon}_\eta E^2C_2},$$

$$A_3 = \frac{s^2(s^2 - \bar{c}^2)[\bar{\epsilon}_\eta\bar{e}_2^2s^2 + \bar{\bar{\epsilon}}(C_2s^2 - \bar{c}^2)]}{C_1C_2E_1 + \bar{\epsilon}_\eta E^2C_2},$$

$$\begin{aligned}R(m_q) = &-\epsilon_P s\{[c_3(\bar{\beta}\bar{\epsilon}_\eta - p) + (\bar{\beta} + pc_1)e_1 - c_1\bar{\epsilon}_\eta - 1]m^4\\ &+[c_3(\bar{\beta}\bar{\epsilon}_\eta\bar{\epsilon} - pe_2) + e_1(pc_2 + \bar{\beta}e_2) - 2e_2 - \bar{\epsilon}_\eta(\bar{\epsilon}c_1 + c_2)s^2 - (pe_1 - \bar{\epsilon}_\eta)c^2]m^2\\ &-s^2[(\bar{\epsilon}_\eta\bar{\epsilon}c_2 + e_2^2)s^2 - \bar{\epsilon}_\eta\bar{\epsilon}c^2]\},\end{aligned}$$

$$\begin{aligned}R_1(m_q) = &\epsilon_P m_q\{c_2(\bar{\beta}\bar{\epsilon}_\eta - p)m^4\\ &+\{[\bar{\beta}\bar{\epsilon}_\eta(\bar{\epsilon}c_2 + 1) + e_1^2\bar{\beta} - p(1 + c_2e_2 - c_3e_1) - (\bar{\epsilon}_\eta c_3 + e_1)]s^2 - (\beta\bar{\epsilon}_\eta - p)c^2\}m^2\\ &+s^2[(s^2 - c^2)(\bar{\beta}\bar{\epsilon}_\eta\bar{\epsilon} - pe_2) - (c_3\bar{\epsilon}_\eta\bar{\epsilon} + e_1e_2)s^2]\},\end{aligned}$$

$$\begin{aligned}R_2(m_q) = &m_q\{(pc_1 + \bar{\beta})c_2m^4 + [p(Ps^2 - Jc^2) + \bar{\beta}(s^2 - c^2) + (e_1c_1 - c_3 + \bar{\beta}e_2c_2 - \bar{\beta}c_3e_1)s^2]m^2\\ &+(s^2 - c^2)[(pc_2 + \bar{\beta}e_2)s^2 - pc^2] + (e_1c_2 - c_3e_2)s^4 - e_1c^2s^2\},\end{aligned}$$

$$\begin{aligned}R_3(m_q) = &\epsilon_P\{c_2(1 + \bar{\epsilon}_\eta c_1)m^6 + [-\{c_3(c_3\bar{\epsilon}_\eta + e_1) + e_1(c_3 - e_1c_1)\}s^2 + (\bar{\epsilon}c_1 + 1)(s^2 - c^2)\\ &+c_2\{c_1\bar{\epsilon}_\eta\bar{\epsilon} + c_2\bar{\epsilon}_\eta + 2e_2)s^2 - \bar{\epsilon}_\eta c^2\}]m^4\\ &+[\{-c_3(c_3\bar{\epsilon}_\eta\bar{\epsilon} + e_1e_2) + e_1(e_1c_2 - e_2c_3)\}s^4 + c_2s^2\{\bar{\epsilon}_\eta\bar{\epsilon}(c_2s^2 - c^2) + e_2^2s^2\}\\ &+(s^2 - c^2)\{(c_1\bar{\epsilon}_\eta\bar{\epsilon} + c_2\bar{\epsilon}_\eta + 2e_2)s^2 - \bar{\epsilon}_\eta c^2\} - e_1^2c^2s^2]m^2\\ &+(s^2 - c^2)s^2\{\bar{\epsilon}_\eta\bar{\epsilon}(c_2s^2 - c^2) + e_2^2s^2\}\},\end{aligned}$$

where

$$C_1 = \frac{(c_1 + \epsilon\bar{\beta}^2)}{1+\epsilon}, \quad C_2 = \frac{c_2}{1+\epsilon}, \quad C_3 = \frac{c_3 + \epsilon\bar{\beta}}{1+\epsilon}, \quad \bar{e}_1 = \frac{e_1 - \epsilon p}{1+\epsilon}, \quad \bar{e}_2 = \frac{e_2}{1+\epsilon},$$

$$E = \frac{(1 - \epsilon\bar{\beta}p)}{1+\epsilon}, \quad \bar{\bar{\epsilon}} = \frac{\bar{\epsilon}}{1+\epsilon}, \quad E_1 = \frac{(1 - \epsilon p^2/\eta_3)}{1+\epsilon}, \quad \bar{c}^2 = \frac{c^2}{1+\epsilon},$$

$$P = c_1 + c_2^2 - c_3^2, \quad J = c_1 + c_2, \quad P' = C_1 + C_2^2 - C_3^2, \quad J' = C_1 + C_2,$$

$$F = \frac{(1+\epsilon)^3C_2(C_1E_1 + \bar{\epsilon}_\eta E^2)}{c_2(c_1 + \bar{\epsilon}_\eta)}.$$

References

[1] R.D. Mindlin, On the equations of motion of piezoelectric crystals, in: Problems of Continuum Mechanics, N.I. Muskelishvili, 70th Birthday Volume, SIAM, Philadelphia, 1961, pp. 282–290.

[2] R.D. Mindlin, Equation of high frequency vibrations of thermo-piezoelectric plates, International Journal of Solids and Structures 10 (1974) 625–637.
[3] W. Nowacki, Some general theorems of thermo-piezoelectricity, Journal of Thermal Stresses 1 (1978) 171–182.
[4] W. Nowacki, Foundations of linear piezoelectricity, in: H. Parkus (Ed.), Electromagnetic Interactions in Elastic Solids, Springer, Wein, 1979 (Chapter 1).
[5] W. Nowacki, Mathematical Modes of Phenomenological Piezoelectricity, New Problems in Mechanics of Continua, University of Waterloo Press, Ontario, 1983, pp. 29–49.
[6] D.S. Chandrasekhariah, A temperature rate dependent theory of piezoelectricity, Journal of Thermal Stresses 7 (1984) 293–306.
[7] D.S. Chandrasekhariah, A generalized linear thermoelasticity theory of piezoelectric media, Acta Mechanica 71 (1988) 39–49.
[8] A.K. Pal, Surface waves in a thermopiezoelectric medium of monoclinic symmetry, Czechoslovakia Journal of Physics 29 (1979) 1271–1281.
[9] A.P. Mayer, Thermoelastic attenuation of surface acoustic waves, International Journal of Engineering Sciences 28 (1990) 1073–1082.
[10] H.S. Paul, K. Ranganatham, Free vibrations of a pyroelectric layer of hexagonal (6 mm) class, Journal of the Acoustical Society of America 78 (1985) 395–397.
[11] H.S. Paul, G.V. Raman, Wave propagation in a hollow pyroelectric circular cylinder of crystal class-6, Acta Mechanica 87 (1991) 37–46.
[12] H.S. Paul, G.V. Raman, Vibrations of pyroelectric plates, Journal of the Acoustical Society of America 90 (1991) 1729–1732.
[13] F. Ashida, T.R. Tauchert, N. Noda, Response of a piezoelectric plate of a crystal class 6 mm subject to axi-symmetric heating, International Journal of Engineering Sciences 31 (1993) 373–384.
[14] E. Radzikowska, Thermopiezoelectricity equation of plates, Bulletin of Academy Polonaise Science Series Sciences Techniques 29 (1981) 195–203.
[15] T.R. Tauchert, Piezothermoelastic behaviour of a laminated plate, Journal of Thermal Stresses 15 (1992) 25–37.
[16] Y.X. Tang, K. Xu, Dynamic analysis of a piezo-thermoelastic laminated plate, Journal of Thermal Stresses 18 (1995) 87–104.
[17] B.A. Martin, S.W. Wenzel, R.M. White, Viscosity and density sensing with ultrasonic plate waves, Sensors and Actuators 1 (1989) 1–6.
[18] E.W. Wenzel, R.M. White, A multisensor employing an ultrasonic Lamb wave oscillator, IEEE Transaction of Electronic Devices 35 (1988) 735–743.
[19] S.W. Wenzel, R.M. White, Analytic comparison of the sensitivities of bulk-wave, surface-wave and flexural plate-wave ultrasonic gravimetric sensors, Applied Physics Letters 54 (1989) 1976–1978.
[20] A. Schoch, Der schalldurchgang durch platten (Sound transmission in plates), Acoustica 2 (1952) 1–17.
[21] J.G. Scholte, On true and pseudo Rayleigh waves, Proceedings of the Koninklijke Nederlandse Akademie van Wetenschappen Series 52 (1949) 652–653.
[22] D. Watkins, W.H.B. Cooper, A.B. Gillespie, R.B. Pike, The attenuation of Lamb waves in the presence of a liquid, Ultrasonics 20 (1982) 257–264.
[23] J. Wu, Z. Zhu, The propagation of Lamb waves in a plate bordered with layers of a liquid, Journal of the Acoustical Society of America 91 (1992) 861–867.
[24] J. Wu, Z. Zhu, The propagation of Lamb waves in a plate bordered with a viscous liquid, Journal of the Acoustical Society of America 98 (1995) 1057–1067.
[25] J.N. Sharma, V. Pathania, Thermoelastic waves in a plate bordered with layers of inviscid liquid, Journal of Thermal Stresses 26 (2002) 149–166.
[26] J.S. Yang, R.C. Batra, Free vibrations of a linear thermo-piezoelectric body, Journal of Thermal Stresses 18 (1995) 247–262.
[27] J.N. Sharma, M. Kumar, Plane harmonic waves in piezo-thermoelastic materials, Indian Journal of Engineering Material Science 7 (2000) 434–442.
[28] J.N. Sharma, On the propagation of thermoelastic waves in homogeneous isotropic plates, Indian Journal of Pure and Applied Mathematics 32 (2001) 1329–1341.